EDMS Id: **841455**

ORGANISATION EUROPEENNE POUR LA RECHERCHE NUCLEAIRE
EUROPEAN ORGANIZATION FOR NUCLEAR RESEARCH

Laboratoire Européen pour la Physique des Particules
European Laboratory for Particle Physics

Safety Commission

Technical Note
CERN-SC-2007-031-RP-TN

Radiation protection considerations for the installation of Linac 4 in the existing Linac 2 building

Matteo Magistris, Egidio Mauro and Marco Silari

Abstract

This note discusses Monte Carlo simulations performed to assess the possibility of installing the Linac 4 accelerator in the Linac 2 building with some additional shielding to the existing structure. The note provides an estimate of the ambient dose equivalent rate $H^*(10)$ in the building 351, housing the Linac 3 accelerator, close to the high energy section of the Linac 2 accelerator, and on the gangway connecting these two buildings that it is not classified as a radiation area.

CERN, 1211 Geneva 23, Switzerland
7 May 2007

1. Introduction

A new proton linac, called Linac 4, is being designed at CERN to replace the present Linac 2 injecting protons at 50 MeV into the PS booster (PSB). Linac 4 will deliver H^- ions at a kinetic energy of 160 MeV (see, for example, ref. [1]) and it is also conceived for use as the front-end of the future multi-GeV, multi-MW Superconducting Proton Linac (SPL) [2, 3]. For its use as PSB injector, Linac 4 will operate at 2 Hz, with a peak current of 40 mA and a pulse length of 0.4 ms. These parameters correspond to 0.08% of the maximum beam duty cycle and 0.032 mA average current or 2 x 10^{14} protons per second, equivalent to a beam power of 5.1 kW at the top energy of 160 MeV.

The overall architecture of Linac 4 is schematically shown in Fig. 1. The ion source is followed by a Radio Frequency Quadrupole (RFQ), a chopper line and the main linear accelerator structure. Three types of accelerating structures bring the energy up to 160 MeV: a Drift Tube Linac (DTL) up to 40 MeV, a Cell-Coupled Drift Tube Linac (CCDTL) up to 90 MeV and finally a Side Coupled Linac (SCL) to the final energy. A long transfer line equipped with debunching and collimation sections connects Linac 4 to the existing Linac 2 transfer line.

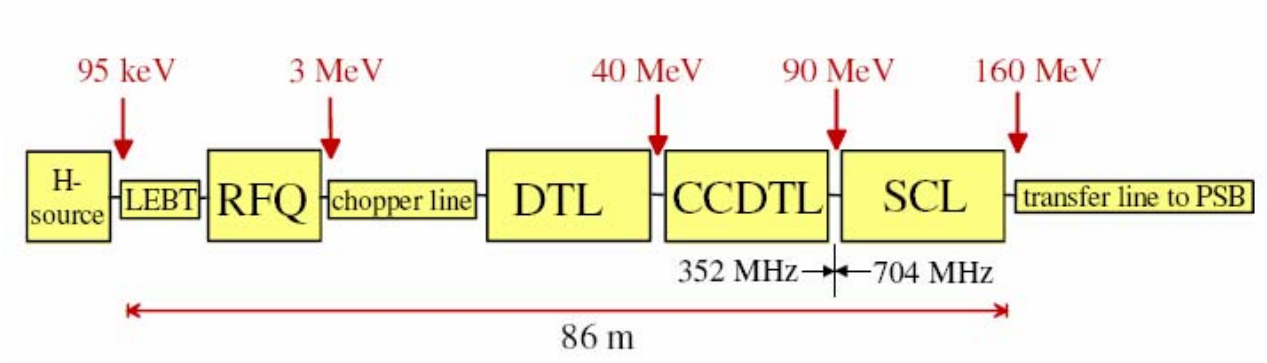

Figure 1: Schematic view of Linac 4.

Four possible locations were considered for the site of Linac 4:
1) the South Hall of the PS complex (discussed in refs. [4, 5 and 6]);
2) the Linac 2 building with a substantial reinforcement of the existing shielding;
3) the Linac 2 building with little additional shielding to the existing structure;
4) a green field solution under the *Mont Citron* close to the Linac2/PS complex.

This note studies, from a radiation protection point of view, the third scenario evaluating the radiological efficiency of the additional shielding by Monte Carlo simulations with the FLUKA [7, 8] radiation transport code.

2. The layout of the simulations

The geometry implemented in the simulations includes the following structures (the height is given with reference to the tunnel floor):

- The part of building 363 housing the high energy (140-160 MeV) section of the accelerator (Fig. 2) consisting of

- the 14 m long, 3.5 m wide and 3.5 m high accelerator tunnel, with the 100 cm thick concrete shield on the left side, an additional 40 cm thick concrete shield on the right side (i.e., towards Linac 3), the 100 cm thick concrete roof (the accelerator beam axis is at 126 cm height)
- the 14 m long service gallery on the left side of the accelerator at 170 cm height
- the 30 cm thick concrete wall on the left side of the service gallery
- the 30 cm thick concrete floor of the accelerator tunnel
- the building roof made of iron (1 cm thickness, 10.6 m height)

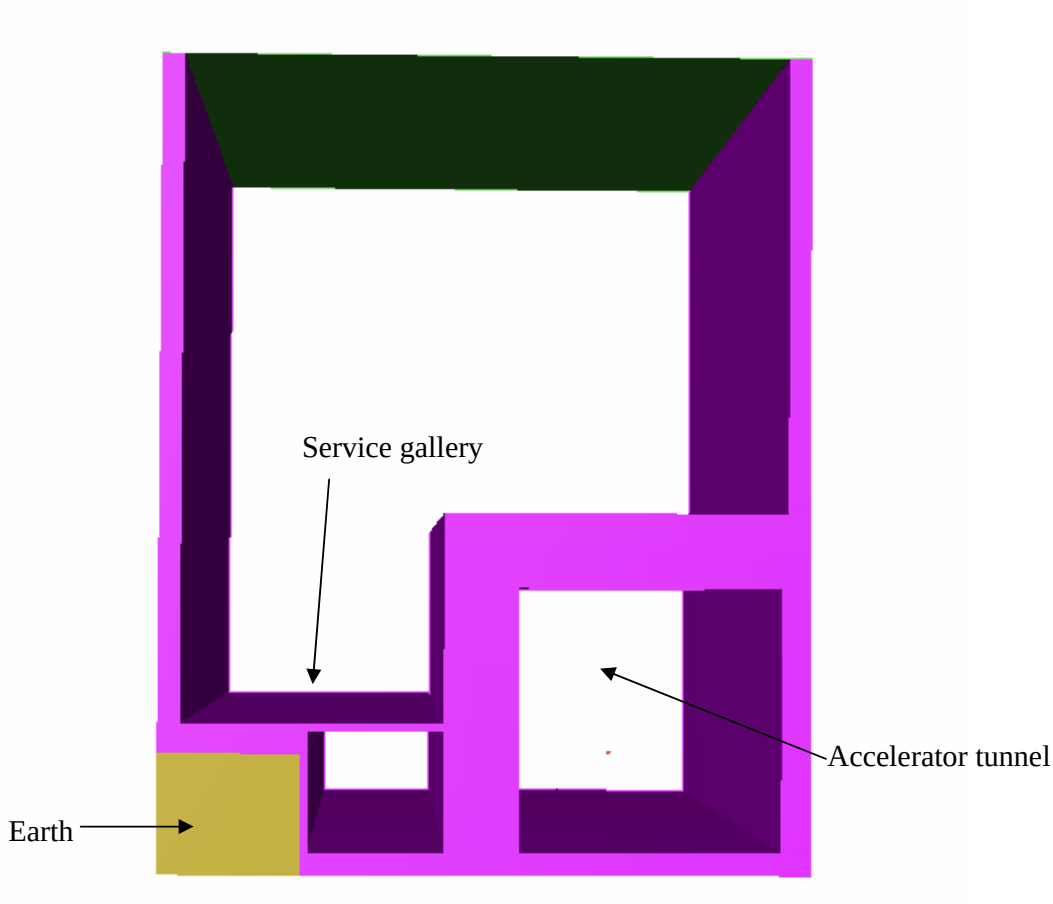

Figure 2: The high-energy section of the Linac 4 tunnel in building 363 as coded in FLUKA and visualised via the SimpleGeo geometry package [9]. The view is looking downstream of the tunnel, towards the transfer line.

- The measurement tunnel (Fig. 3), which corresponds to the first part of the transfer line, consisting of:

  - the 8.6 m long, 3.5 m wide and 6.1 m high measurement tunnel, with the 100 cm thick concrete shield on the left side, an additional 40 cm thick concrete shield on the right side and the 100 cm thick concrete roof
  - the 30 cm thick concrete floor
  - the 8.6 m long, 1.5 m wide and 5.5 m high tunnel on the left side of the measurement tunnel with the 20 cm thick concrete roof and the 20 cm thick concrete wall

- the earth above these tunnels, up to 650 cm height in the first metre and 750 cm height in the remaining 7.6 metres (consequently the first metre of the measurement tunnel is not underground).

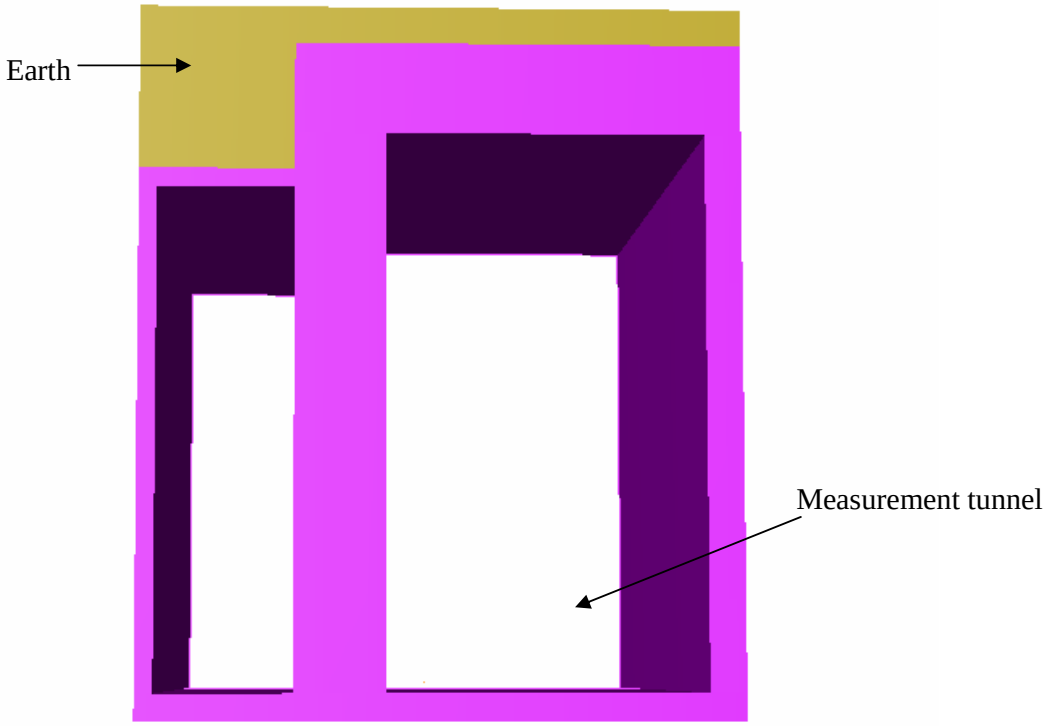

Figure 3: SimpleGeo [9] view of the measurement tunnel in building 363. The view is looking downstream of the tunnel in the beam direction.

- The second part of the transfer tunnel (Fig. 4) (i.e., downstream of the measurement tunnel) consisting of

  - the 3.3 m long, 3.5 m wide and 2.5 m high initial section, with the 100 cm thick concrete shield on the left side, an additional 40 cm thick concrete shield on the right side, the 100 cm thick concrete roof
  - the 30 cm thick concrete floor
  - the 5.5 m high and 6.3 m wide part of this building housing the tunnel with a 20 cm thick concrete roof and a 20 cm thick concrete left wall
  - the earth up to 750 cm height

- The building 351 housing the linac 3 accelerator and the earth between building 351 and building 363 (Fig. 5) consisting of

  - the wall of the building 50 cm thick, made of concrete and tilted with respect to the shield on the right side of the linac 2 accelerator tunnel
  - the first part of building 351 (closest to the first 10 metres of the linac 2 tunnel), which is 750 cm high and it is not underground, while the second part (closest to the final part of the accelerator and the transfer line) is 570 cm high and it is underground
  - the earth between the two buildings, defined as a tilted plane with respect to the floor of the accelerator, in the first 14 metres reaching a maximum height of 610 cm, 650 cm high between 14 and 15 metres and 750 cm high in the remaining part

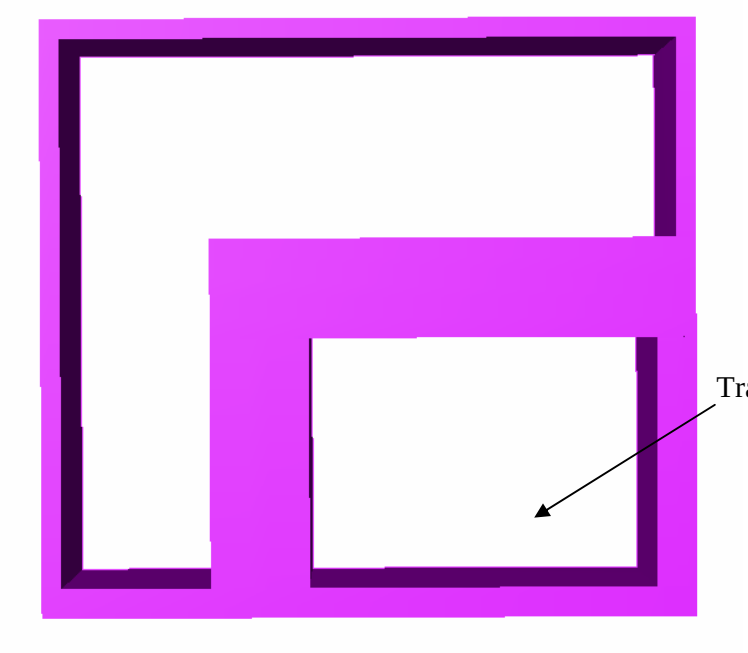

Figure 4: SimpleGeo [9] view of the transfer line tunnel. The view is looking downstream of the tunnel, towards the high-energy end of the linac.

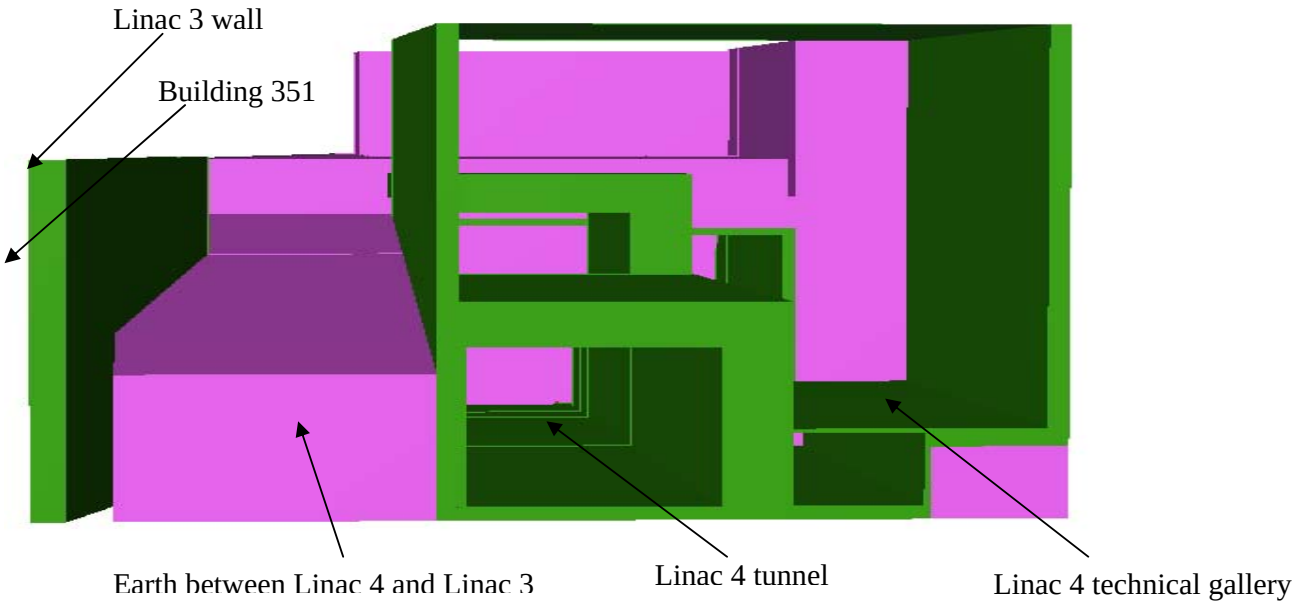

Figure 5: SimpleGeo [9] front view of the Linac 4 building and the wall of building 351. The view is looking upstream of the tunnel, towards the high-energy end of the linac.

3. Biasing techniques

Region-importance biasing techniques were used to improve the statistical accuracy of the results. Between the beam loss point and building 351 the region importance factor was increased by 1.6 each 10 cm of concrete and by 4.8 each 49 cm of earth. This factor was assessed by simple estimates taking into account the radiation attenuation in concrete and in earth.

4. Stray radiation in building 351 adjacent to the Linac 2 building

A routine loss of 1 W/m was assumed as guideline value in the shielding calculations. In a real scenario, beam losses will most likely not be equally distributed along the machine, but rather concentrated in a number of "hot spots". As for the previous studies, for the present calculations it was assumed that constant losses of 10 W occur at selected points along the machine and in term of shielding design, this assumption is almost equivalent to 10 W loss uniformly distributed over 10 m [4, 5 and 6].

As shown in Fig. 6, one the most critical issues with the installation of Linac 4 in the Linac 2 building, is its proximity with building 351 housing Linac 3, the ion injector. At present Linac 3 is shielded from the Linac 2 radiation with molasse (from 3 to 6 m thickness, depending on location). The section of Linac 4 closest to building 351 is where the energy increases from 140 to 160 MeV.

The high energy section and the transfer line of Linac 4 were modelled quite precisely with FLUKA. The earth shielding separating the accelerator from Linac 3 was implemented with the actual thickness, whilst a 40 cm thick layer of concrete was added to the adjacent Linac 4 wall to improve the shielding without major changes in the building structure. The earth used in the simulations is molasse with a density of 2.4 g/cm^3 and with the following composition: O (49,5%), Si (19,8%), Al (6,4%), K (1,8%), Fe (3,9%), Mg (3,2%), Na (0,5%), Ca (9,3%), Mn (0,1%) and C (5%).

In all cases a proton beam hitting a 5 x 5 x 5 cm^3 copper target was considered, to simulate a point loss in a thick target, such as a quadrupole or a drift tube. Copper was chosen as a material also representative of other elements with similar density (e.g., iron and stainless steel).

The same FLUKA geometry was used for two separate sets of simulations, namely to predict the prompt radiation in building 351 near the high energy section and the transfer line.

The first critical situation studied is the stray radiation in the part of building 351 close to the 140 MeV section of Linac 4. The ambient dose equivalent rate H*(10) was scored on the ground floor of building 351, where the Linac 3 technical gallery is situated, and at an height between 490 cm and 570 cm, where the gangway on the first floor is located.

As shown in the Fig. 7, for point losses in Linac 4 of 10 W every 10 m, the dose rate in this part of the technical gallery is less than 1 μSv/h. On the contrary, the dose rate at the gangway on the first floor can reach a maximum value of 100 μSv/h (Fig. 8). The reason for this high dose rate can be ascribed to the insufficient amount of earth shielding present between these two buildings (Fig. 5)

In the second simulation the stray radiation in the part of building 351 close to the transfer line of Linac 4 was studied. The ambient dose equivalent rate H*(10) was scored on the ground floor (Fig. 9) and on the first floor of building 351 (Fig. 10) and, in addition, at an height between 730 cm and 810 cm, corresponding to the level of the roof of the building, where the gangway connecting the two buildings is situated (Fig. 11).

In this part of the building, the dose rate in the technical gallery is less than 0.1 µSv/h and on the gangway on the first floor is less than 1 µSv/h. The simulations showed that the situation on the gangway connecting building 363 and building 351 is critical, as the dose rate reaches a maximum of 100 µSv/h and, moreover, this gangway is accessible to the members of the public.

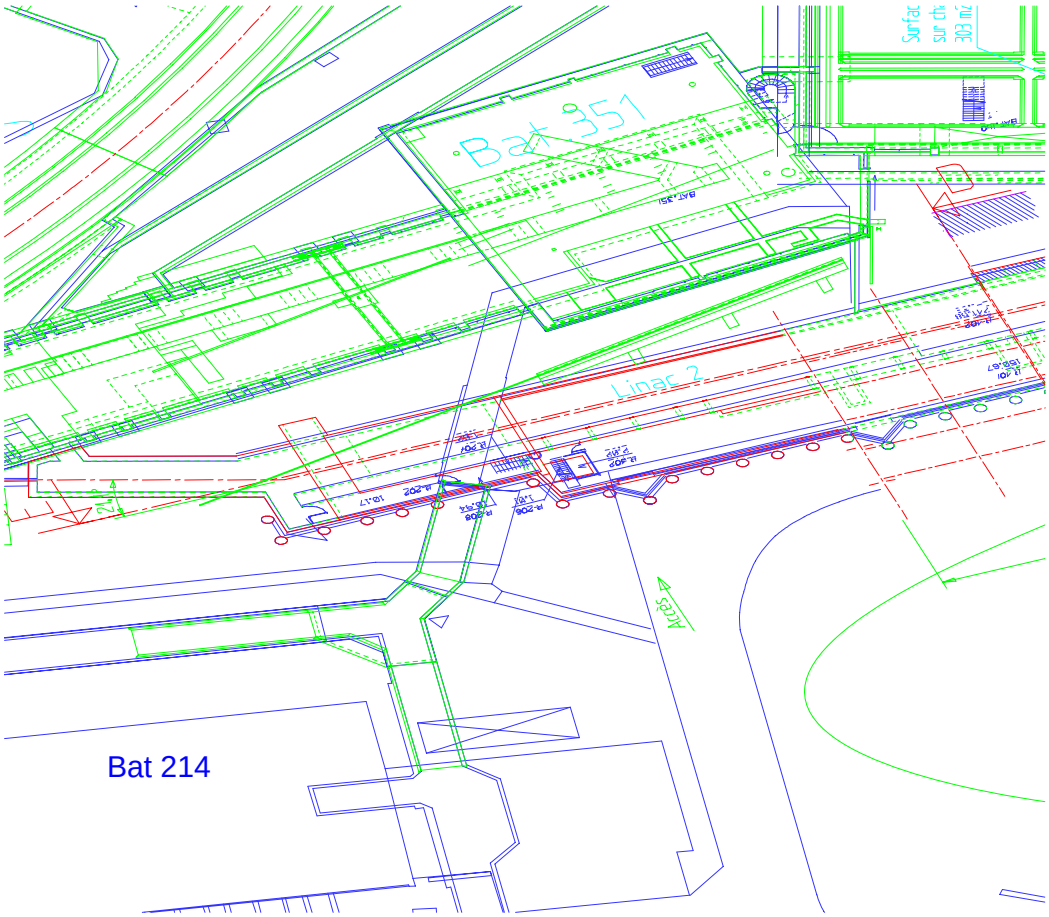

Figure 6: Bird's-eye view of Linac 2 and of the adjacent buildings.

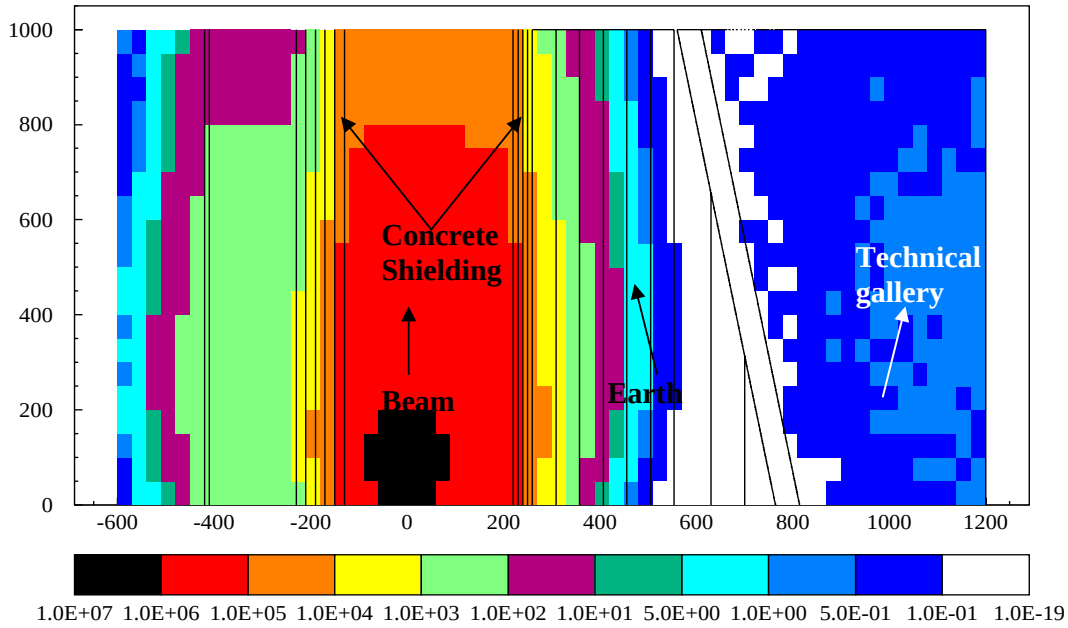

Figure 7: Beam loss in a 5 x 5 x 5 cm^3 copper target, 10 W, 140 MeV. Top cross sectional view of the Linac 4 tunnel and of building 351. H*(10) in µSv/h on the ground floor.

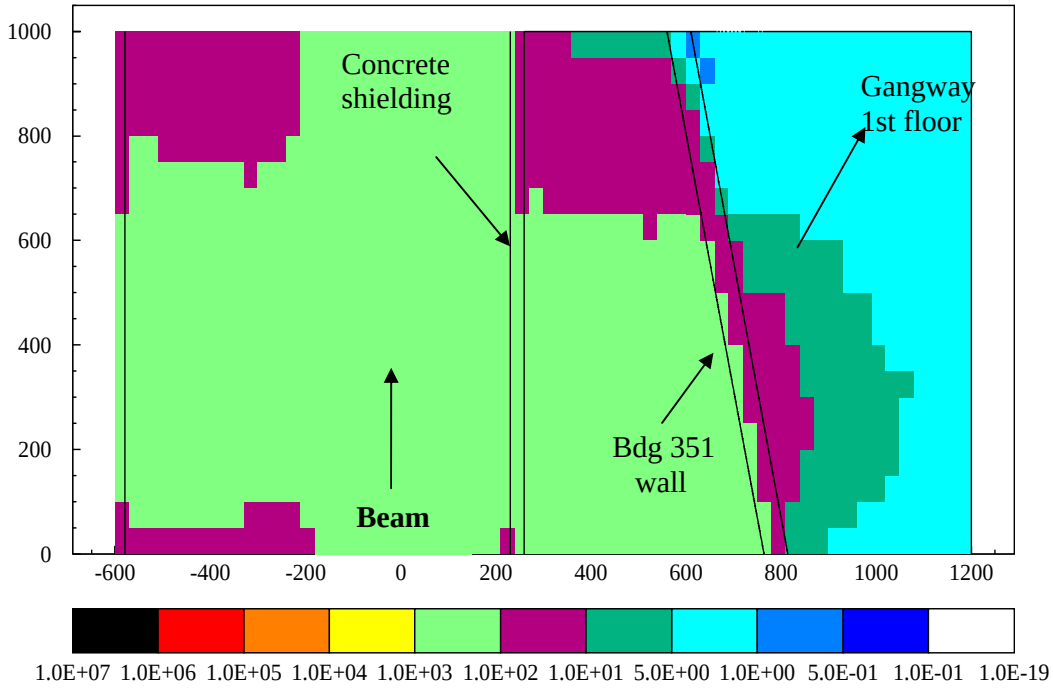

Figure 8: Beam loss in a 5 x 5 x 5 cm^3 copper target, 10 W, 140 MeV. Top cross sectional view of the Linac 4 tunnel and of building 351. H*(10) in µSv/h at 530 cm above the hall floor where the gangway is located.

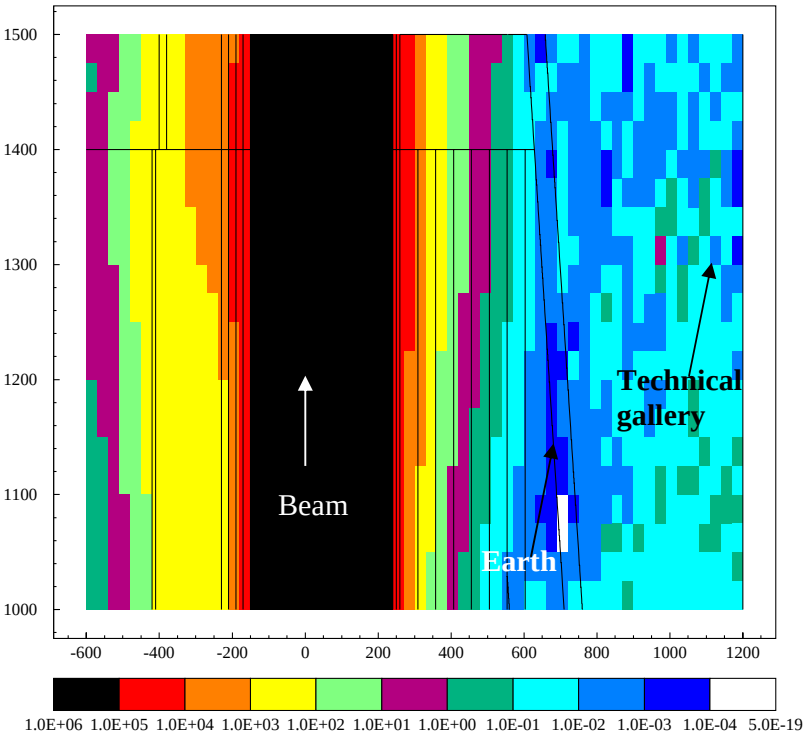

Figure 9: Beam loss in a 5 x 5 x 5 cm^3 copper target, 10 W, 160 MeV. Top cross sectional view of the Linac 4 tunnel and of building 351. H*(10) in µSv/h on the ground floor where the Linac 3 technical gallery is located.

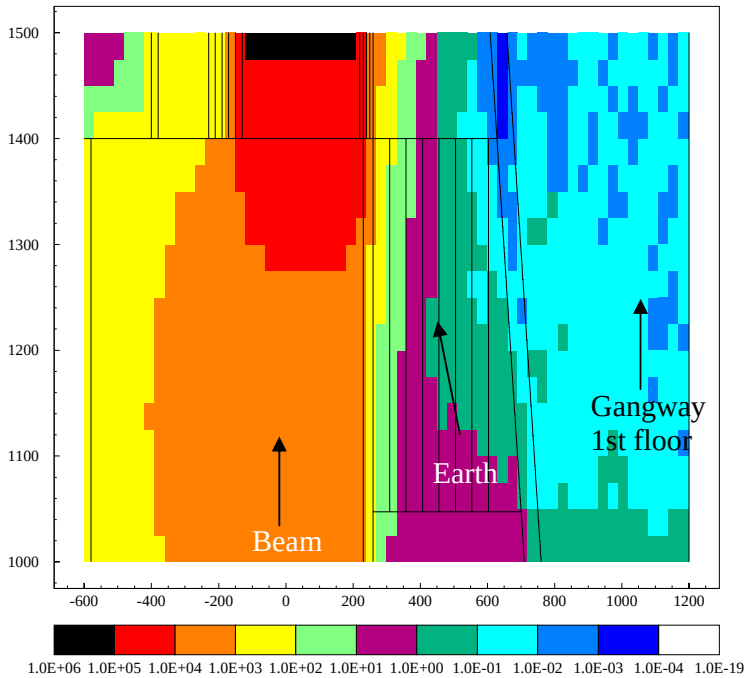

Figure 10: Beam loss in a 5 x 5 x 5 cm^3 copper target, 10 W, 160 MeV. Top cross sectional view of the Linac 4 tunnel and of building 351. H*(10) in µSv/h at 530 cm above the hall floor where the gangway is located.

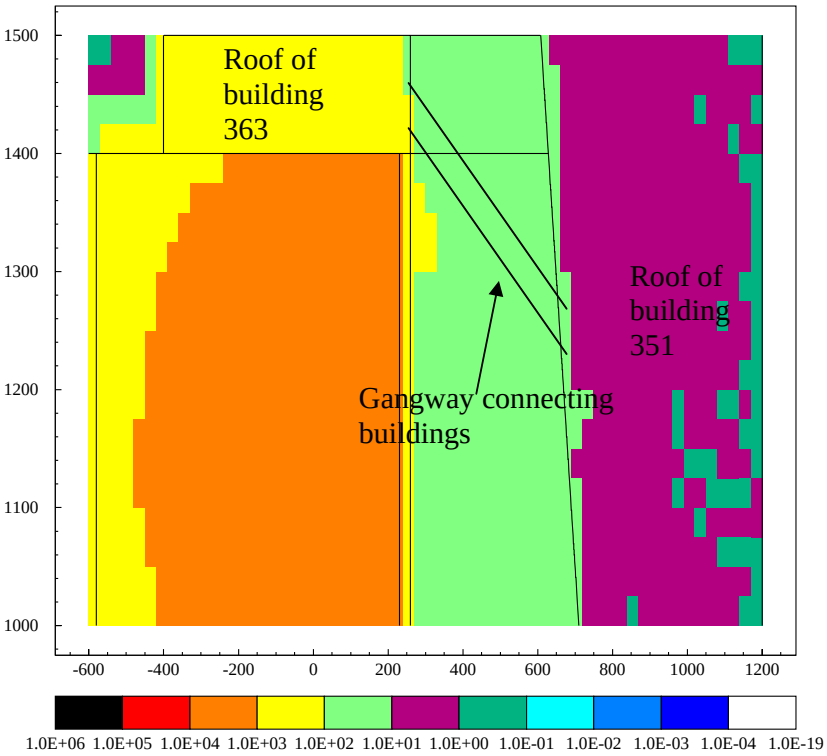

Figure 11: Beam loss in a 5 x 5 x 5 cm^3 copper target, 10 W, 160 MeV. Top cross sectional view of the Linac 4 tunnel and of building 351. H*(10) in µSv/h at 760 cm above the hall floor where the gangway connecting the two buildings is located.

6. Conclusions

Monte Carlo simulations were performed to study the possibility of installing Linac 4 in the building presently housing the Linac 2 accelerator, with some additional concrete shielding in the direction of the Linac 3 accelerator hall.

The simulations showed two critical situations: on the gangway connecting building 363 and building 351 and on the gangway on the first floor of building 351, where the dose equivalent rate can reach a maximum value of 100 µSv/h.

The existing amount of earth and the additional 40 cm thick layer of concrete between the Linac 3 and Linac 4 are inadequate for reducing the dose rate to a value compatible with the CERN Safety Code [10] in all occupied areas. This problem could be partially solved by using additional earth to completely fill the gap between the two buildings, up to 750 cm height. Further study would be needed to assess the presence of other weak points in the shielding.

The present study did not take into account the stray radiation coming from the PS and the radiation coming from Linac 3 itself, which also contributes to the dose rate in building 351. This aspect, which is negligible with respect to the radiation from Linac 4 in the present conditions, should be studied at a further stage of the shielding design.

References

[1] L. Arnaudon et al, *Linac 4 Technical Design Report*, M. Vretenar and F. Gerick, Editors, CERN-2006-AB-084 (2006).

[2] B. Autin et al., *Conceptual design of the SPL, a high power superconducting H– linac at CERN*, CERN Yellow Report 2000-012 (2000).

[3] F. Gerigk et al., *Conceptual design of the SPL II*, CERN Yellow Report 2006-006 (2006).

[4] M. Magistris and M. Silari, *Preliminary shielding design of Linac 4*, CERN-SC-2005-011-RP-TN (2005).

[5] M. Magistris and M. Silari, *Preliminary shielding design of Linac 4. Top shielding and induced radioactivity*, CERN-SC-2005-050-RP-TN (2005).

[6] M. Magistris, E. Mauro and M. Silari, *Complementary shielding calculation for Linac 4 in the South Hall*, CERN-SC-2006-060-RP-TN (2006).

[7] A. Fasso`, A. Ferrari, J. Ranft, and P.R. Sala, *FLUKA: a multi-particle transport code*, CERN-2005-10 (2005), INFN/TC_05/11, SLAC-R-773.

[8] A. Fasso`, A. Ferrari, S. Roesler, P.R. Sala, G. Battistoni, F. Cerutti, E. Gadioli, M.V. Garzelli, F. Ballarini, A. Ottolenghi, A. Empl and J. Ranft, *The physics models of FLUKA: status and recent developments*, Computing in High Energy and Nuclear Physics 2003 Conference (CHEP2003), La Jolla, CA, USA, March 24-28, 2003, (paper MOMT005), eConf C0303241 (2003), arXiv:hep-ph/0306267.

[9] C. Theis, K.H. Buchegger, M. Brugger, D. Forkel-Wirth, S. Roesler and H. Vincke, *Interactive three dimensional visualization and creation of geometries for Monte Carlo calculations*, Nucl. Instrum. and Meth. A 562, 827-829 (2006).

[10] Safety Code F, Radiation Protection (November 2006).